The local dark matter distribution from hydrodynamic simulations

Nassim Bozorgnia

GRAPPA Institute
University of Amsterdam

Based on work done with F. Calore, M. Lovell, G. Bertone, and the EAGLE team

arXiv: 1601.04707

GRAPPA
GRavitation AstroParticle Physics Amsterdam

UNIVERSITY OF AMSTERDAM

Dark matter halo

- Very little is known about the details of the dark matter (DM) halo in the local neighborhood. $\Rightarrow$ *significant uncertainty when interpreting data from direct detection experiments.*

Dark matter halo

- Very little is known about the details of the dark matter (DM) halo in the local neighborhood. $\Rightarrow$ *significant uncertainty when interpreting data from direct detection experiments.*
- Usually the Standard Halo Model is assumed: isothermal sphere with an isotropic Maxwell-Boltzmann velocity distribution.
  - local DM density: $\rho_\chi \sim 0.3$ GeV cm^{-3}
  - typical DM velocity: $\bar{v} \simeq 220$ km/s

Dark matter halo

- Very little is known about the details of the dark matter (DM) halo in the local neighborhood. $\Rightarrow$ *significant uncertainty when interpreting data from direct detection experiments.*
- Usually the Standard Halo Model is assumed: isothermal sphere with an isotropic Maxwell-Boltzmann velocity distribution.
  - local DM density: $\rho_\chi \sim 0.3$ GeV cm^{-3}
  - typical DM velocity: $\bar{v} \simeq 220$ km/s
- Numerical simulations of galaxy formation predict dark matter velocity distributions which can deviate from a Maxwellian.

Dark matter direct detection

- Strong tension between hints for a signal and exclusion limits:

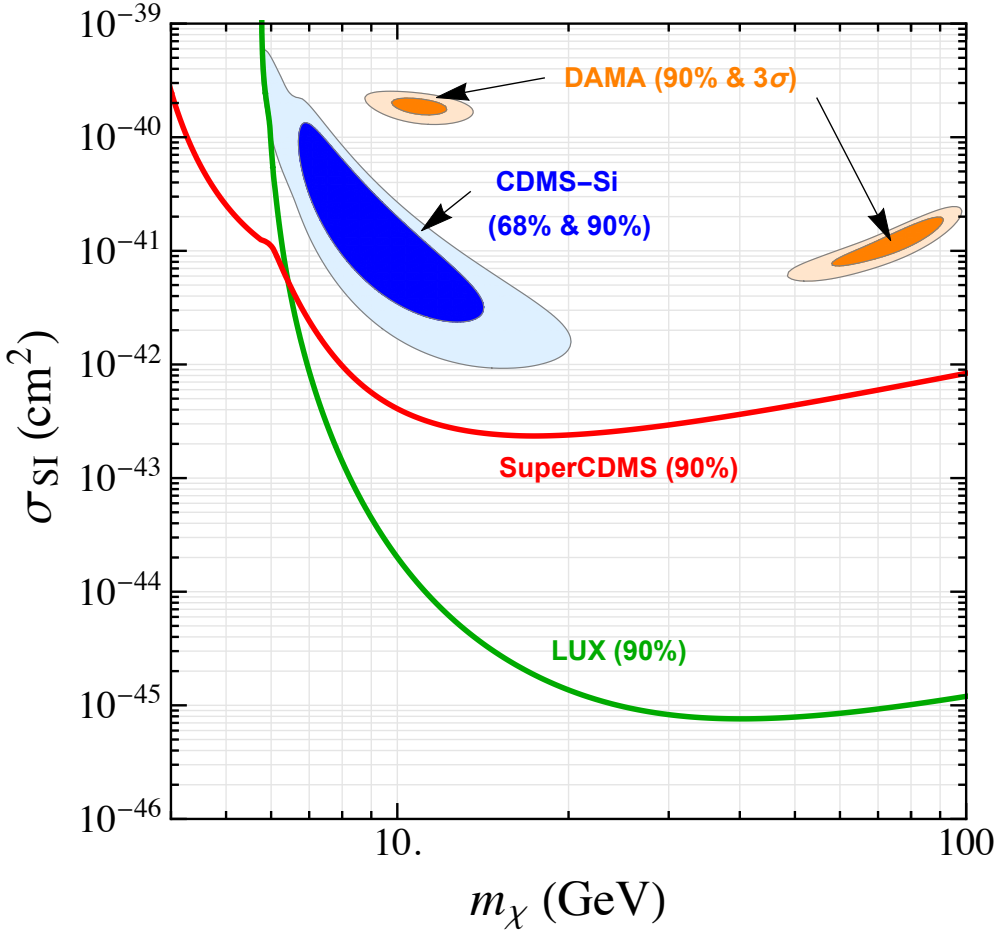

- These kinds of plots assume the Standard Halo Model and a specific DM-nucleus interaction.

Our aim

- Identify Milky Way-like galaxies in high resolution hydrodynamic simulations, by taking into account observational constraints on the Milky Way (MW).
- Extract the local DM density and velocity distribution for the selected MW analogues.
- Analyze the data from direct detection experiments, using the predicted local DM distributions of the selected haloes.

Hydrodynamic simulations

- The **EAGLE** and **APOSTLE** hydrodynamic simulations (**DM** $+$ **baryons**) at two different resolutions.

Name	L (Mpc)	N	$m_{\rm g}$ $(\mathrm{M}_\odot)$	$m_{\rm dm}$ $(\mathrm{M}_\odot)$
EAGLE IR	100	6.8×10^9	1.81×10^6	9.70×10^6
EAGLE HR	25	8.5×10^8	2.26×10^5	1.21×10^6
APOSTLE IR	–	–	1.3×10^5	5.9×10^5

Hydrodynamic simulations

- The **EAGLE** and **APOSTLE** hydrodynamic simulations (**DM** + **baryons**) at two different resolutions.

Name	L (Mpc)	N	$m_{\rm g}$ ($\rm M_\odot$)	$m_{\rm dm}$ ($\rm M_\odot$)
EAGLE IR	100	6.8×10^9	1.81×10^6	9.70×10^6
EAGLE HR	25	8.5×10^8	2.26×10^5	1.21×10^6
APOSTLE IR	–	–	1.3×10^5	5.9×10^5

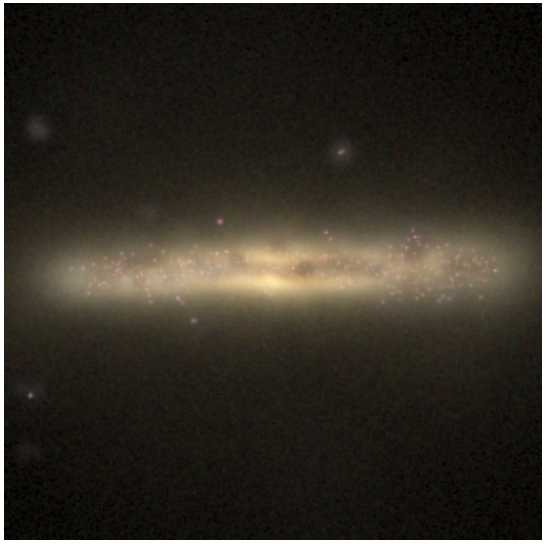

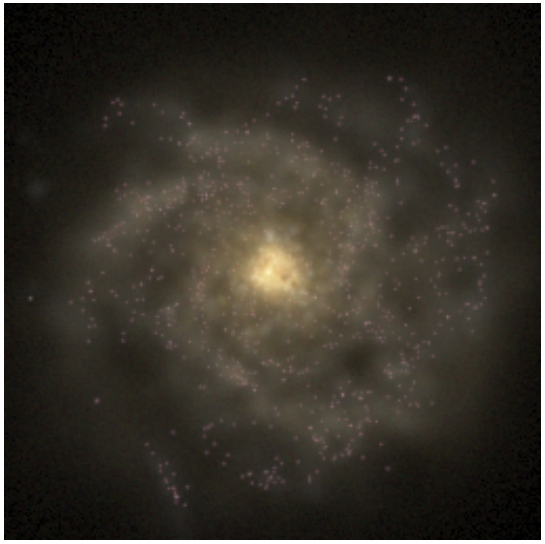

These simulations are calibrated to reproduce the observed distribution of stellar masses and sizes of low-redshift galaxies.

Hydrodynamic simulations

- The **EAGLE** and **APOSTLE** hydrodynamic simulations (**DM** + **baryons**) at two different resolutions.

Name	L (Mpc)	N	$m_{\rm g}$ ($\rm M_\odot$)	$m_{\rm dm}$ ($\rm M_\odot$)
EAGLE IR	100	6.8×10^9	1.81×10^6	9.70×10^6
EAGLE HR	25	8.5×10^8	2.26×10^5	1.21×10^6
APOSTLE IR	–	–	1.3×10^5	5.9×10^5

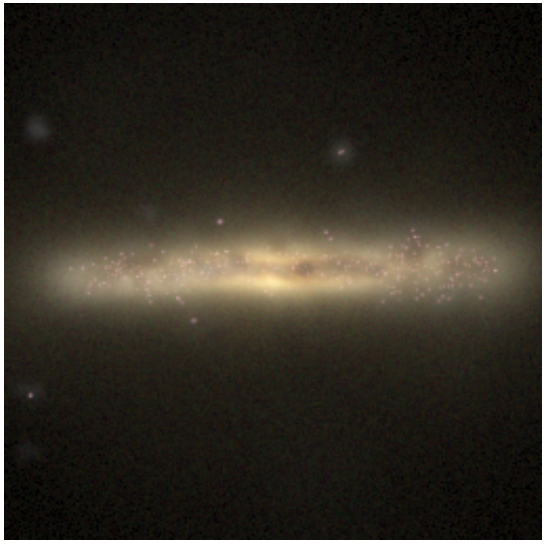

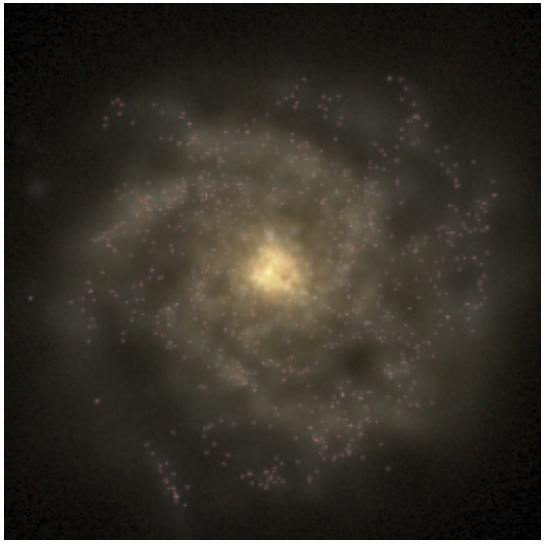

These simulations are calibrated to reproduce the observed distribution of stellar masses and sizes of low-redshift galaxies.

- Companion dark matter only (DMO) simulations were run assuming all the matter content is collisionless.

Identifying Milky Way analogues

- Usually a simulated halo is classified as *MW-like* if it satisfies the MW mass constraint, which has a large uncertainty. We show that the mass constraint is not enough to define a MW-like galaxy.

Identifying Milky Way analogues

- Usually a simulated halo is classified as *MW-like* if it satisfies the MW mass constraint, which has a large uncertainty. We show that the mass constraint is not enough to define a MW-like galaxy.
- Consider simulated haloes with $5 \times 10^{11} < M_{200}/\mathrm{M}_\odot < 2 \times 10^{13}$ and select the galaxies which most closely resemble the MW by the following criteria:
  - Rotation curve from simulation fits well the observed MW kinematical data from: [Iocco, Pato, Bertone, 1502.03821].
  - The total stellar mass of the simulated galaxies is within the 3σ observed MW range: $4.5 \times 10^{10} < M_*/\mathrm{M}_\odot < 8.3 \times 10^{10}$.

Observations vs. simulations

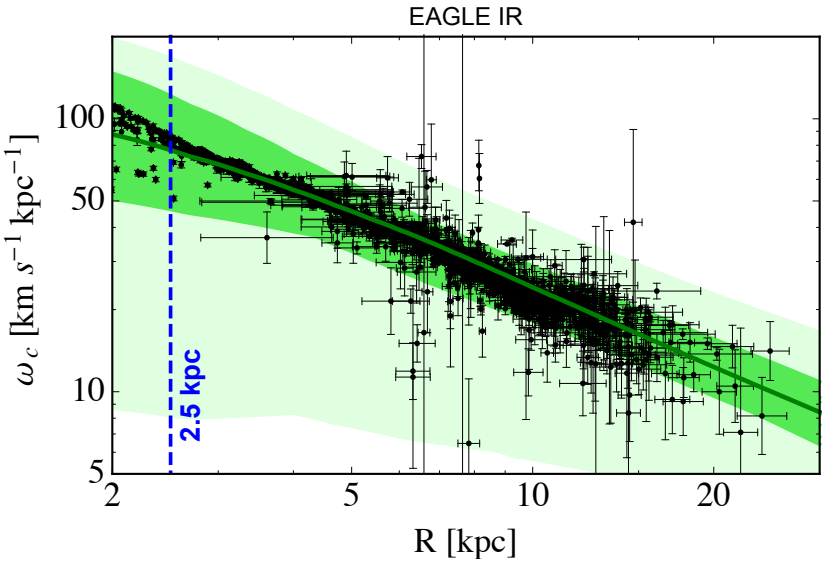

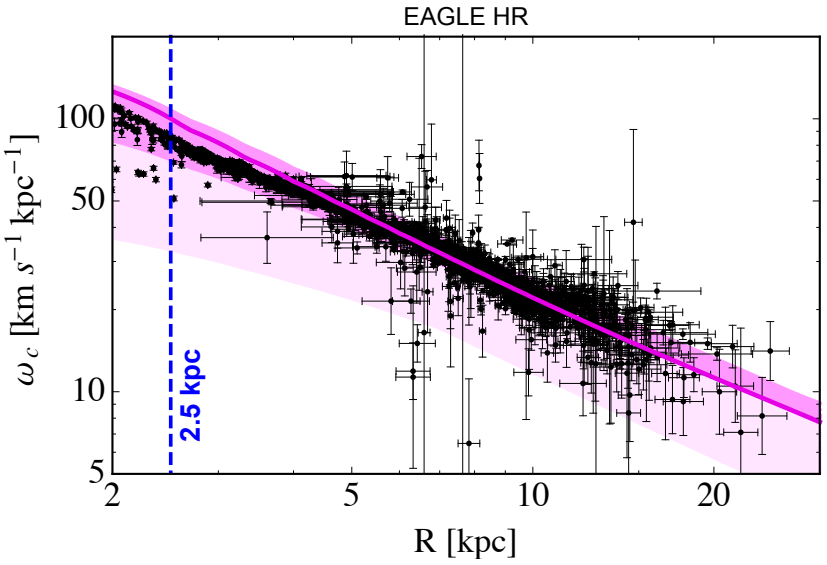

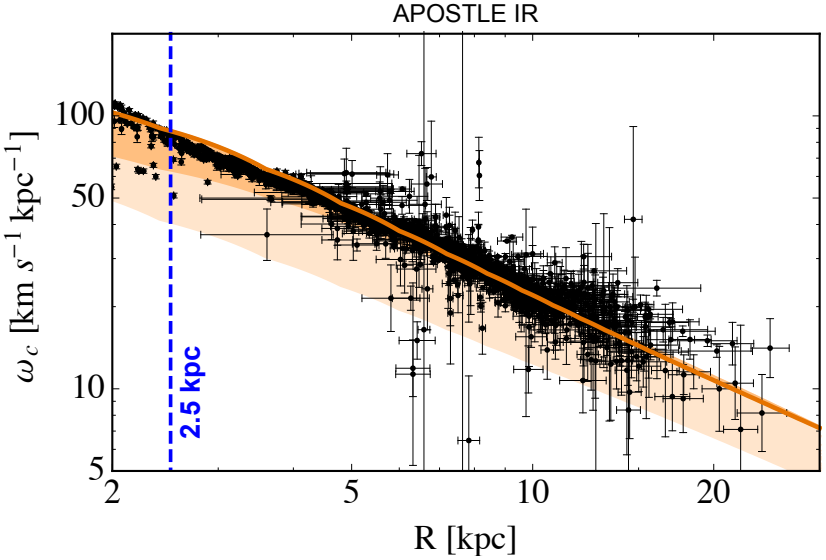

Initial sets of haloes:

EAGLE IR: 2411 | **EAGLE HR: 61** | **APOSTLE IR: 24**

Haloes which have correct total stellar mass:

EAGLE IR: 335 | **EAGLE HR: 12** | **APOSTLE IR: 2**

Observations vs. simulations

Goodness of fit to the observed data:

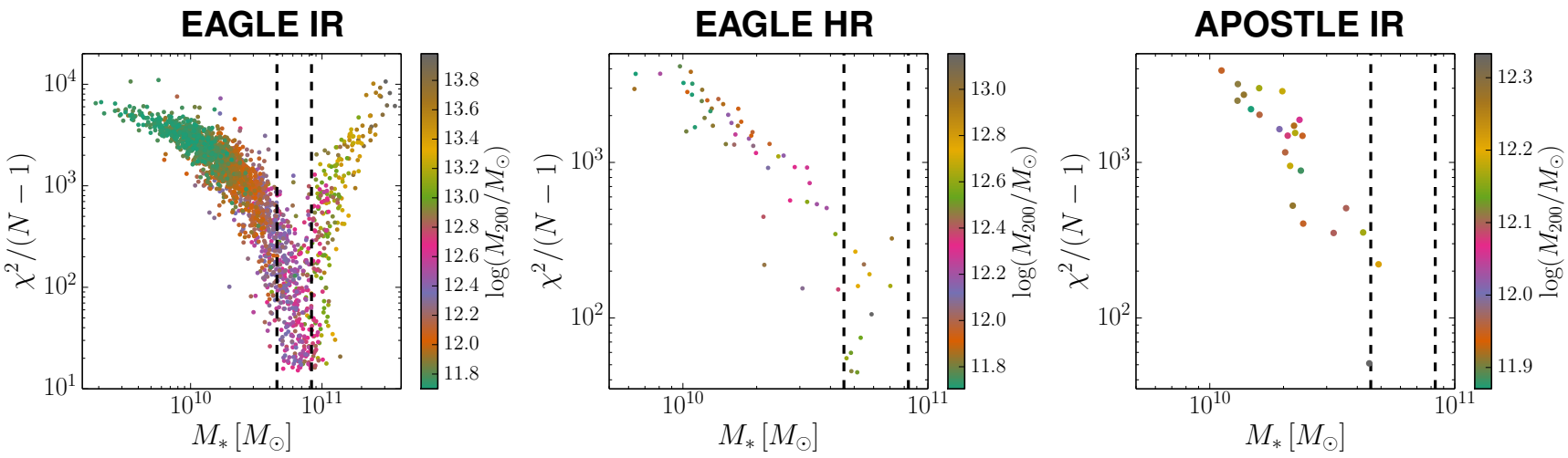

$N = 2687$ is the total number of observational data points used.

- Minimum of the reduced χ^2 occurs within the 3σ measured range of the MW total stellar mass. $\Rightarrow$ haloes with correct MW stellar mass have rotation curves which match well the observations.

Observations vs. simulations

Goodness of fit to the observed data:

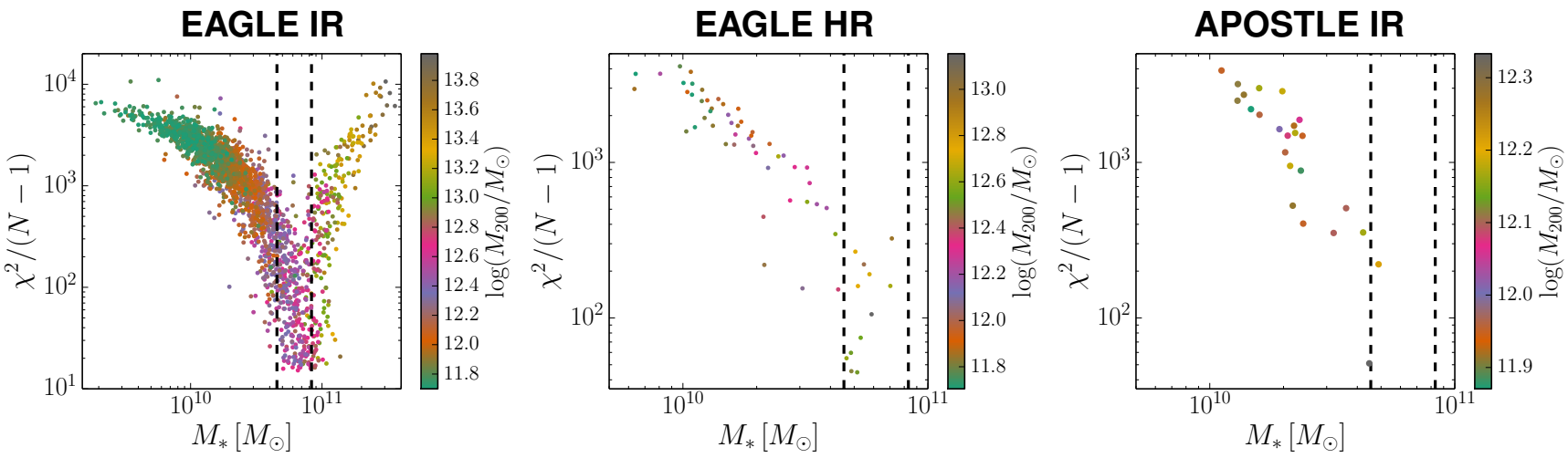

$N = 2687$ is the total number of observational data points used.

- Minimum of the reduced χ^2 occurs within the 3σ measured range of the MW total stellar mass. $\Rightarrow$ haloes with correct MW stellar mass have rotation curves which match well the observations.
- We focus only on the selected **EAGLE HR** and **APOSTLE IR** haloes due to higher resolution $\Rightarrow$ total of **14** MW analogues.

Dark matter density profiles

- Spherically averaged DM density profiles:

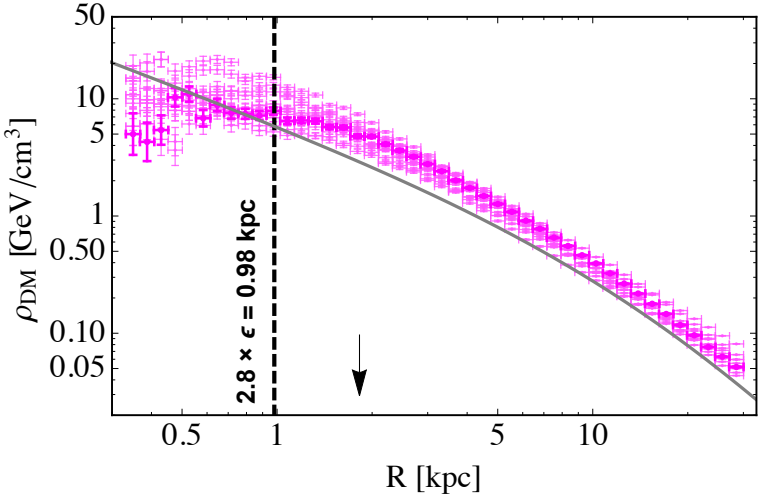

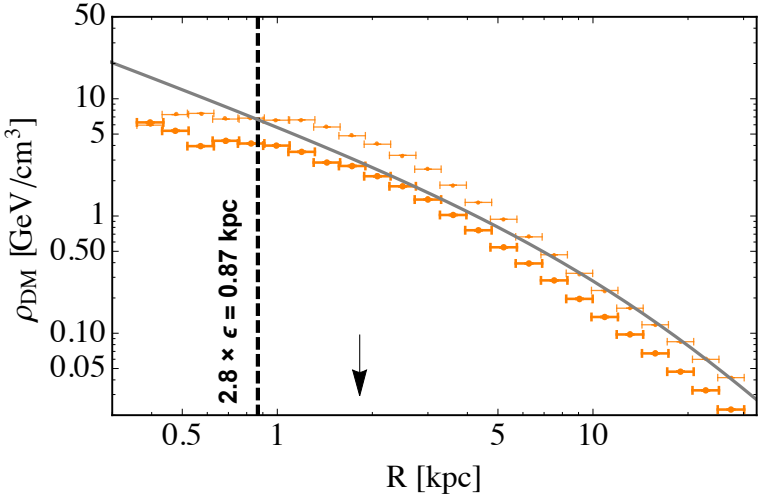

Dark matter density profiles

- Spherically averaged DM density profiles:

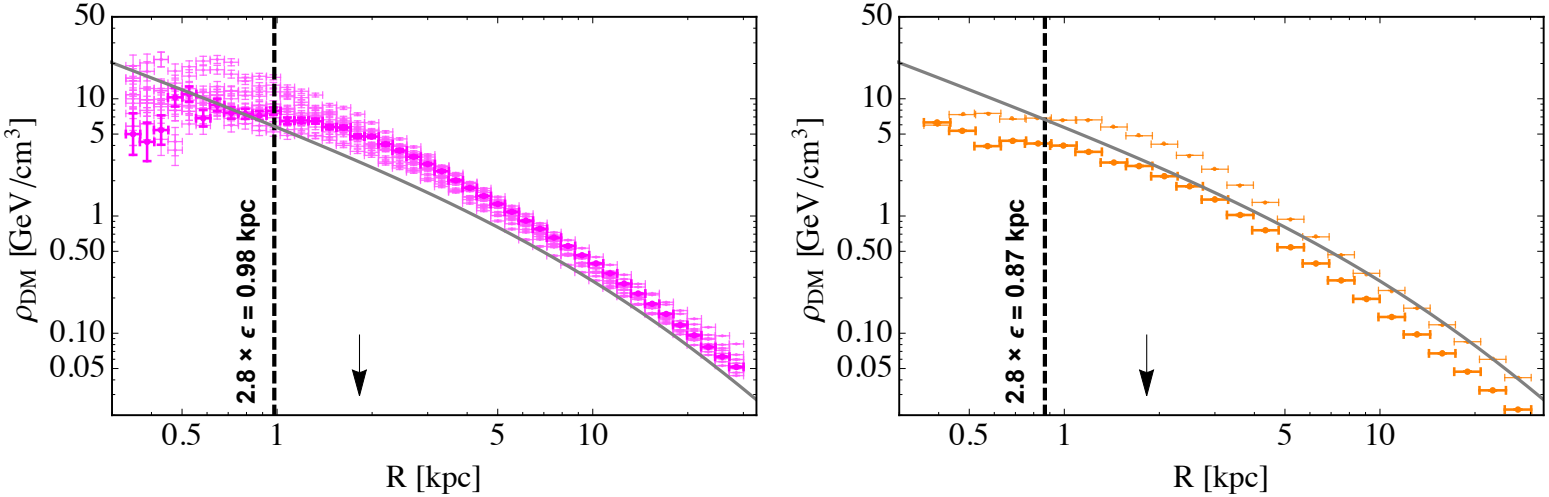

- Need the DM density at the position of the Sun.
- Consider a torus aligned with the stellar disc with $7\ \mathrm{kpc} < R < 9\ \mathrm{kpc}$, and $-1\ \mathrm{kpc} < z < 1\ \mathrm{kpc}$.

EAGLE HR: local $\rho_{\mathrm{DM}} = 0.42 - 0.73$ GeV cm^{-3}.

APOSTLE IR: local $\rho_{\mathrm{DM}} = 0.41 - 0.54$ GeV cm^{-3}.

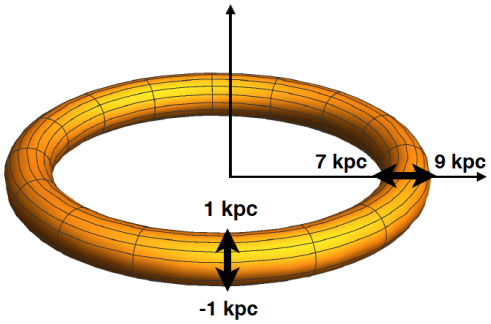

Local speed distributions

In the galactic rest frame:

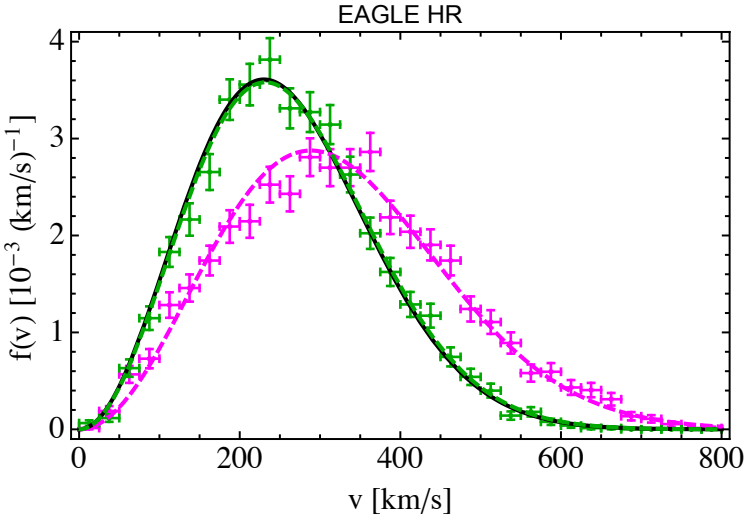

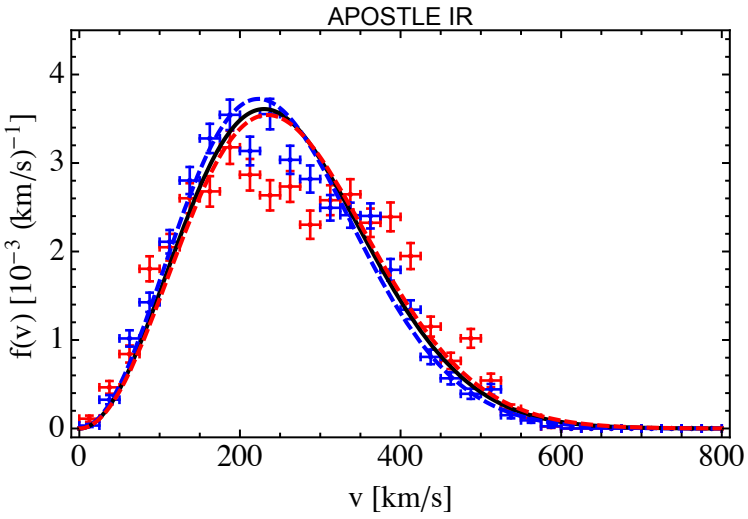

Local speed distributions

In the galactic rest frame:

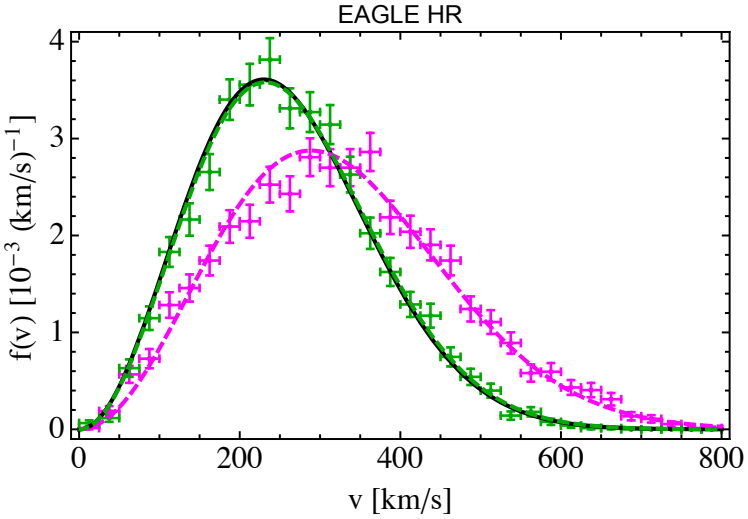

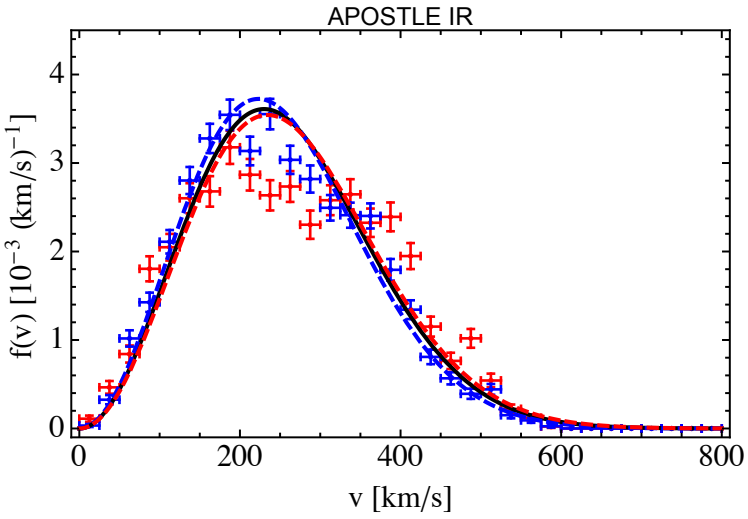

- Comparison to DMO simulations:

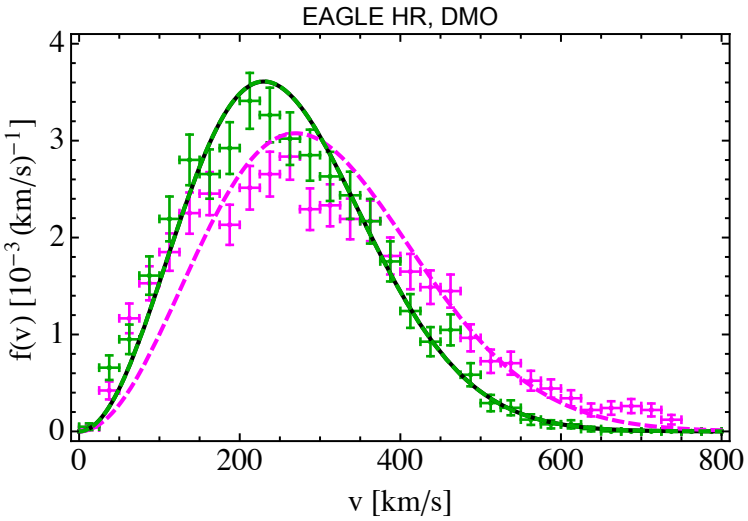

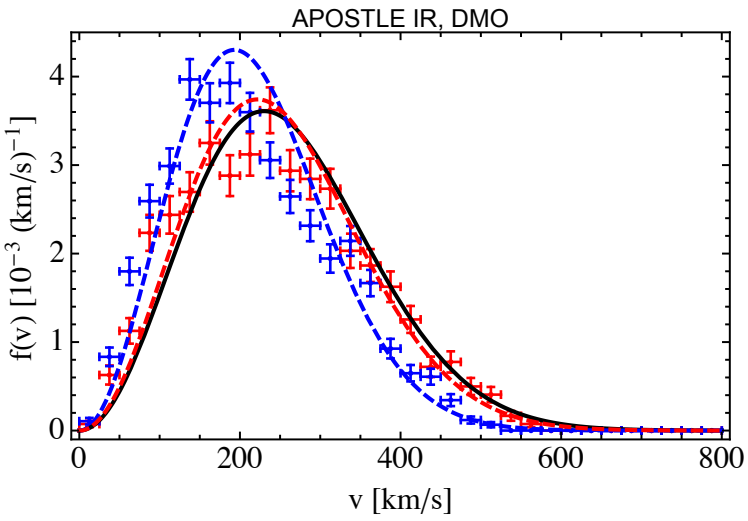

Local DM speed distribution

- Baryons deepen the gravitational potential of the Galaxy in the inner regions, resulting in more high velocity particles. $\Rightarrow$ The peak of the DM speed distribution is shifted to higher speeds when baryons are included in the simulations.

Local DM speed distribution

- Baryons deepen the gravitational potential of the Galaxy in the inner regions, resulting in more high velocity particles. $\Rightarrow$ The peak of the DM speed distribution is shifted to higher speeds when baryons are included in the simulations.
- The Maxwellian distribution with a free peak provides a better fit to most haloes in the hydrodynamic simulations compared to their DMO counterparts.

Local DM speed distribution

- Baryons deepen the gravitational potential of the Galaxy in the inner regions, resulting in more high velocity particles. $\Rightarrow$ The peak of the DM speed distribution is shifted to higher speeds when baryons are included in the simulations.
- The Maxwellian distribution with a free peak provides a better fit to most haloes in the hydrodynamic simulations compared to their DMO counterparts.
- The best fit peak speed of the Maxwellian distribution in the hydrodynamic simulations: 223 – 289 km/s.

Components of the velocity distribution

Distributions of radial, azimuthal, and vertical velocity components:

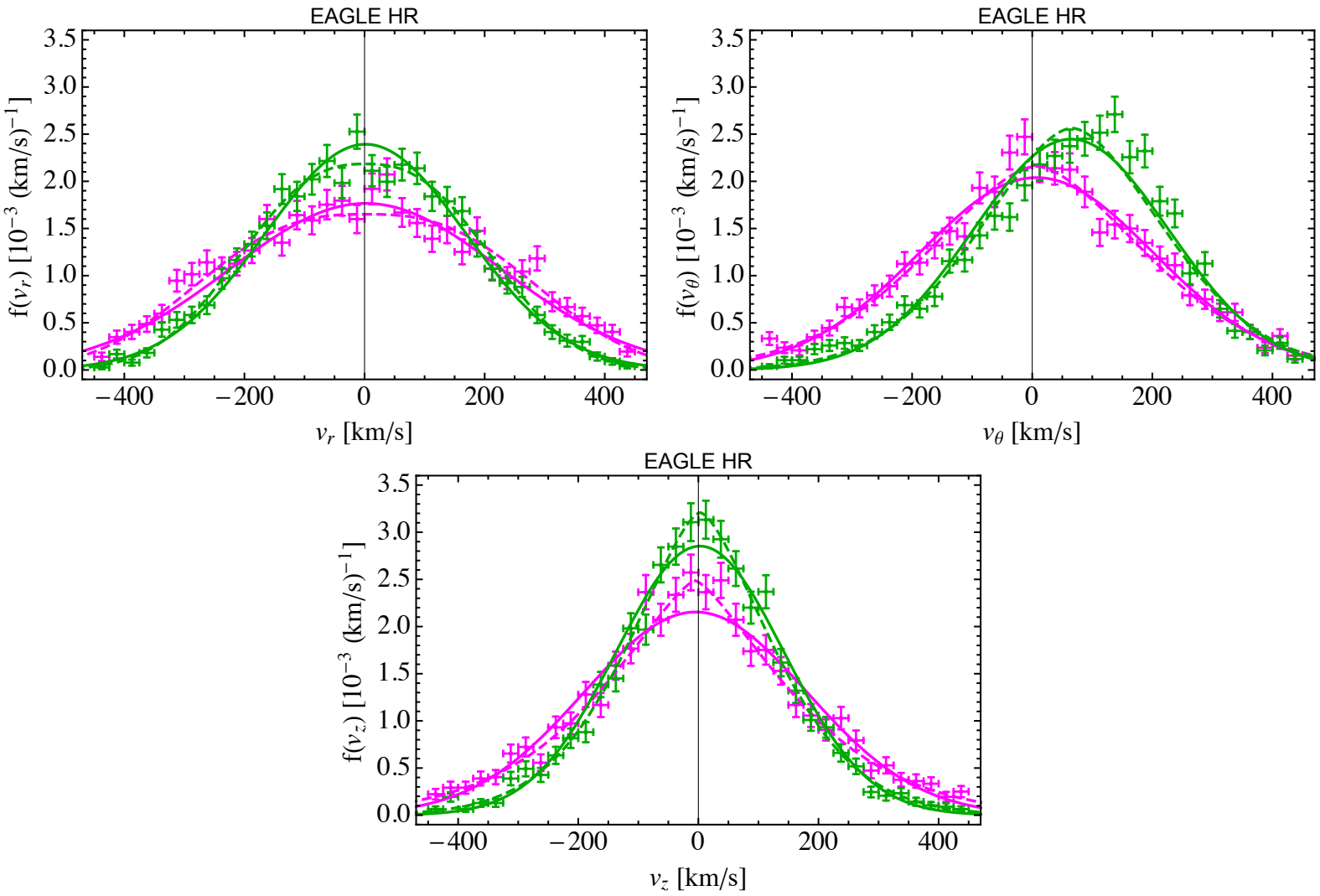

Components of the velocity distribution

Comparison to DMO simulations:

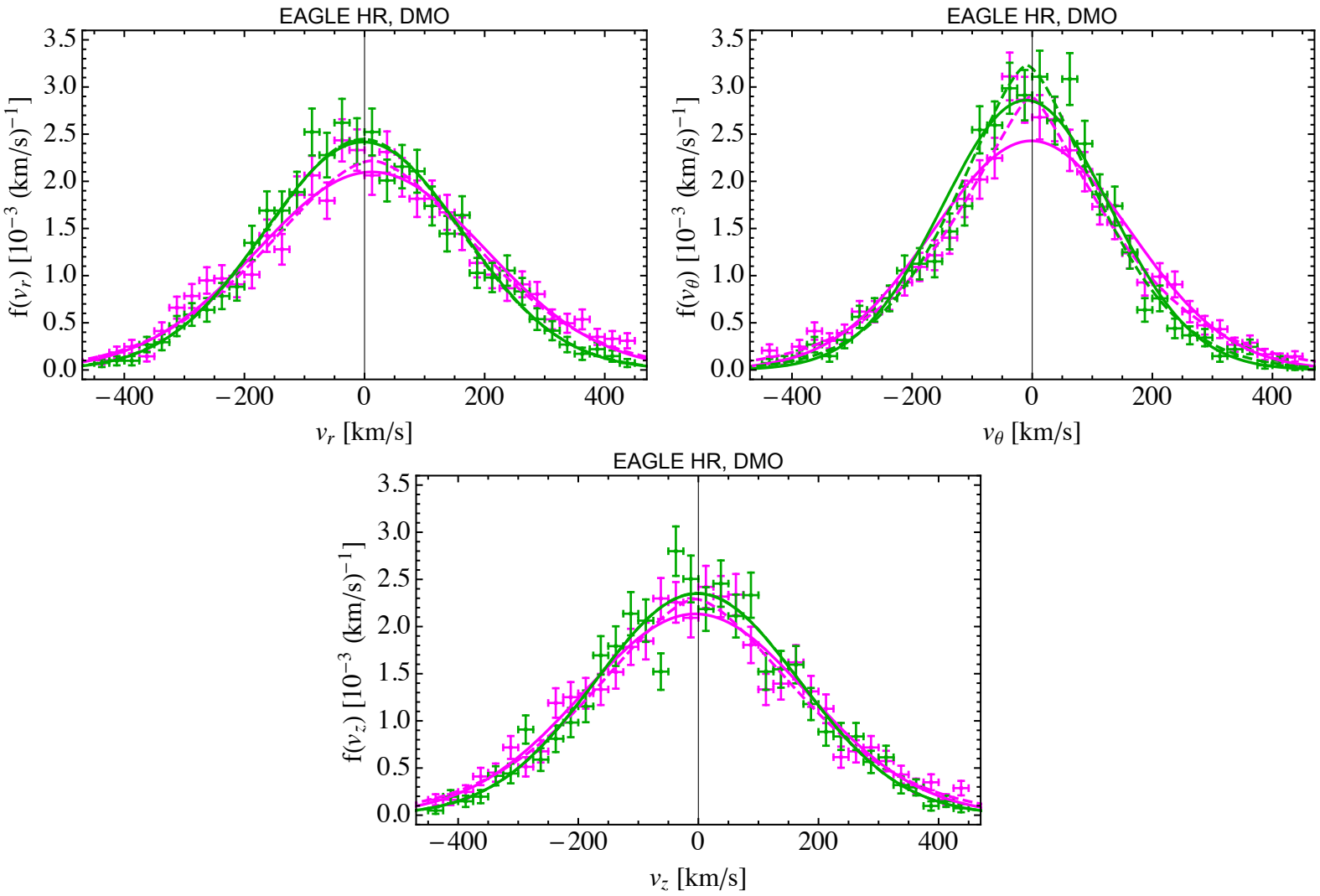

Components of the velocity distribution

- The three components of the DM velocity distribution are not similar. $\Rightarrow$ clear velocity anisotropy at the Solar circle.
- The distributions of the **radial** and **vertical** velocity components are peaked around zero.

Components of the velocity distribution

- The three components of the DM velocity distribution are not similar. $\Rightarrow$ clear velocity anisotropy at the Solar circle.
- The distributions of the **radial** and **vertical** velocity components are peaked around zero.
- Four haloes have a significant positive mean **azimuthal** speed ($\mu > 20$ km/s). The DMO counterparts of these haloes don't show evidence of rotation.

Components of the velocity distribution

- The three components of the DM velocity distribution are not similar. $\Rightarrow$ clear velocity anisotropy at the Solar circle.
- The distributions of the **radial** and **vertical** velocity components are peaked around zero.
- Four haloes have a significant positive mean **azimuthal** speed ($\mu > 20$ km/s). The DMO counterparts of these haloes don't show evidence of rotation.
- Is this pointing to the existence of a "dark disc"?
  - Among the four rotating haloes, two haloes have a rotating DM component in the disc with mean velocity comparable (within 50 km/s) to that of the stars.
  - Hint for the existence of a co-rotating dark disc in two out of 14 MW-like haloes. $\Rightarrow$ dark discs are relatively rare in our halo sample.

The differential event rate

- The differential event rate (event/keV/kg/day):

$$R(E_R, t) = \frac{\rho_\chi}{m_\chi} \frac{1}{m_A} \int_{v>v_m} d^3v \frac{d\sigma_A}{dE_R}\, v\, f_{\rm det}(\mathbf{v}, t)$$

where $v_m = \sqrt{m_A E_R/(2\mu_{\chi A}^2)}$ is the minimum WIMP speed required to produce a recoil energy E_R.

The differential event rate

- The differential event rate (event/keV/kg/day):

$$R(E_R, t) = \frac{\rho_\chi}{m_\chi} \frac{1}{m_A} \int_{v>v_m} d^3v \frac{d\sigma_A}{dE_R}\, v\, f_{\rm det}(\mathbf{v}, t)$$

where $v_m = \sqrt{m_A E_R/(2\mu_{\chi A}^2)}$ is the minimum WIMP speed required to produce a recoil energy E_R.

- For the standard spin-independent and spin-dependent scattering:

$$R(E_R, t) = \underbrace{\frac{\sigma_0\, F^2(E_R)}{2 m_\chi \mu_{\chi A}^2}}_{\text{particle physics}} \underbrace{\rho_\chi\, \eta(v_m, t)}_{\text{astrophysics}}$$

where

$$\boxed{\eta(v_m, t) \equiv \int_{v>v_m} d^3v\, \frac{f_{\rm det}(\mathbf{v}, t)}{v}}$$

halo integral

The halo integral

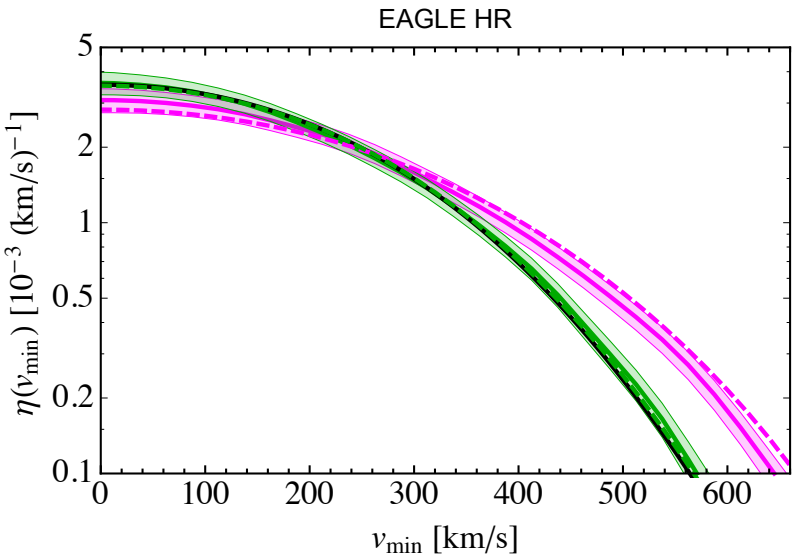

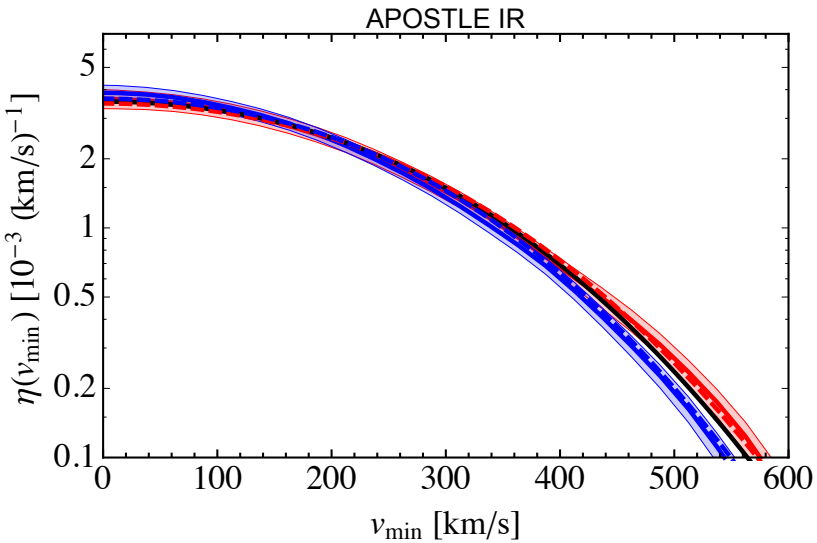

The halo integral

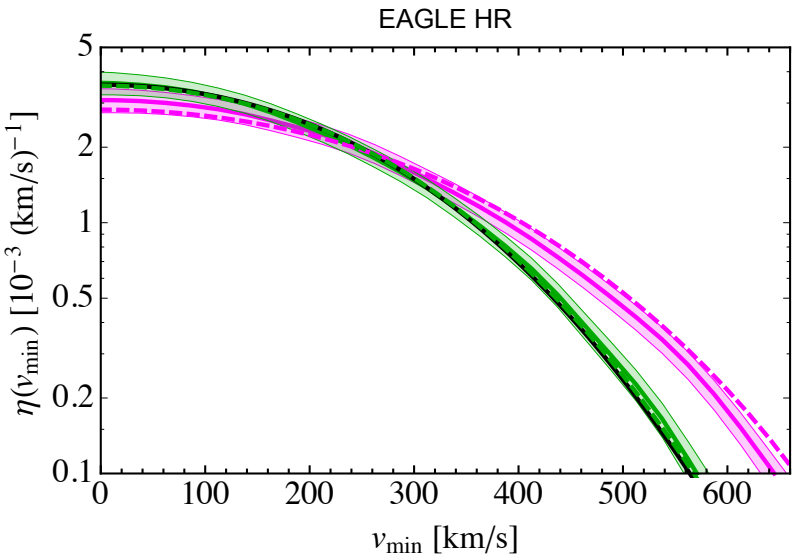

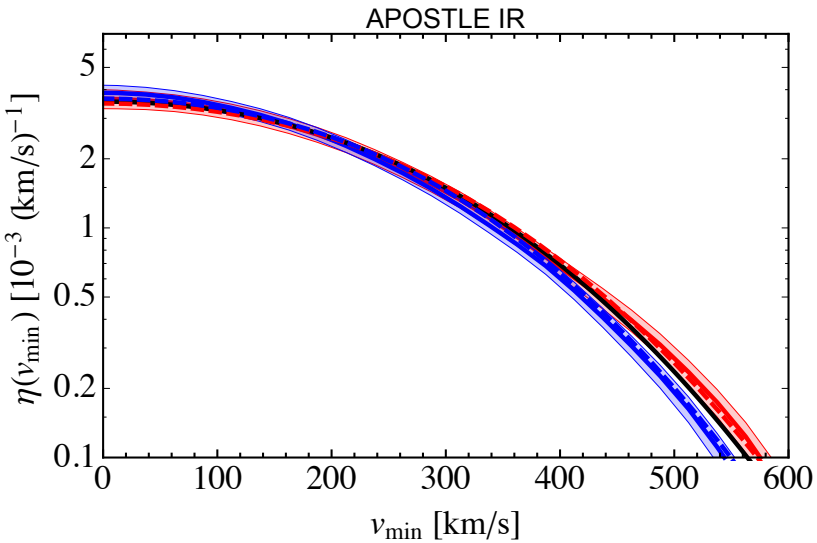

- Significant halo-to-halo scatter in the halo integrals.

The halo integral

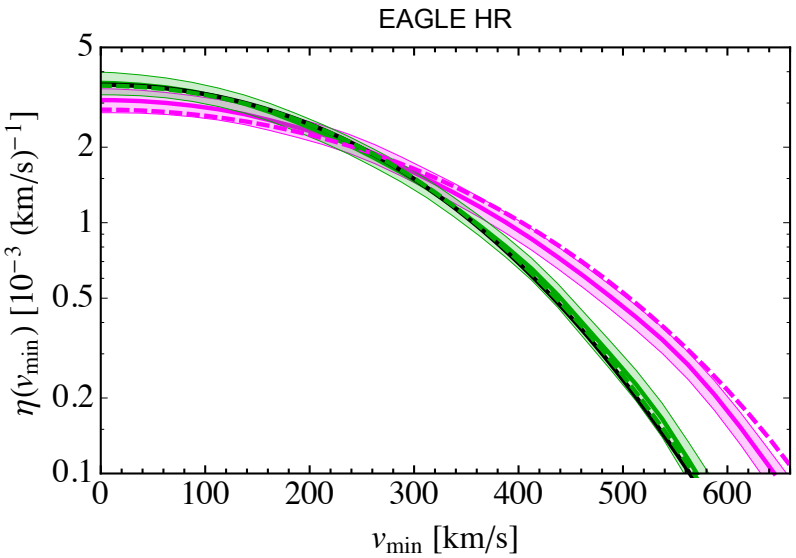

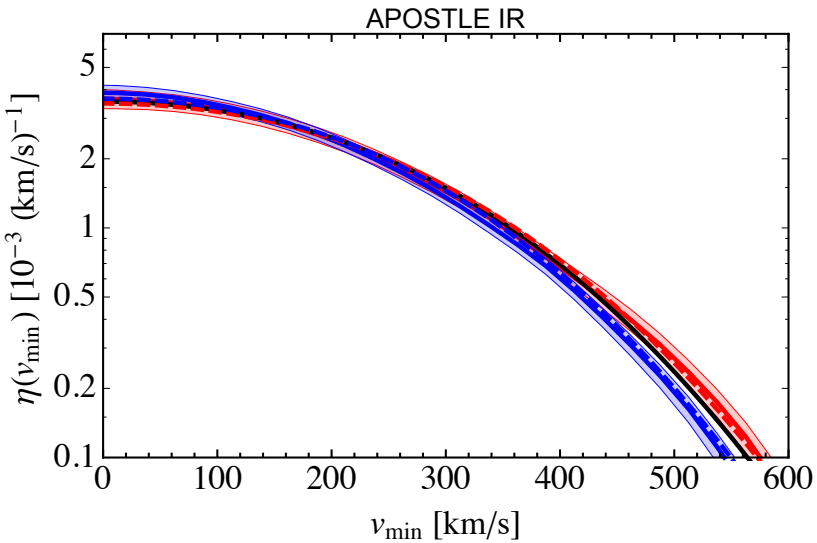

- Significant halo-to-halo scatter in the halo integrals.
- Halo integrals for the best fit Maxwellian velocity distribution (peak speed 223 – 289 km/s) fall within the 1σ uncertainty band of the halo integrals of the simulated haloes.

The halo integral

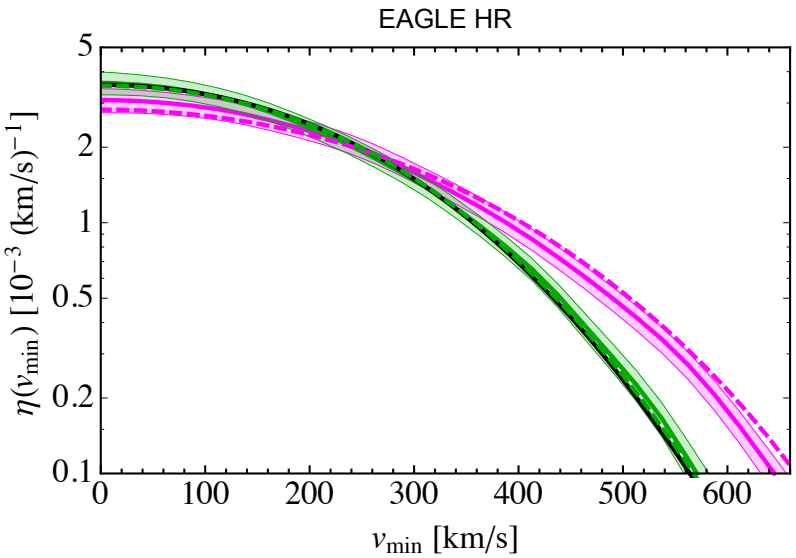

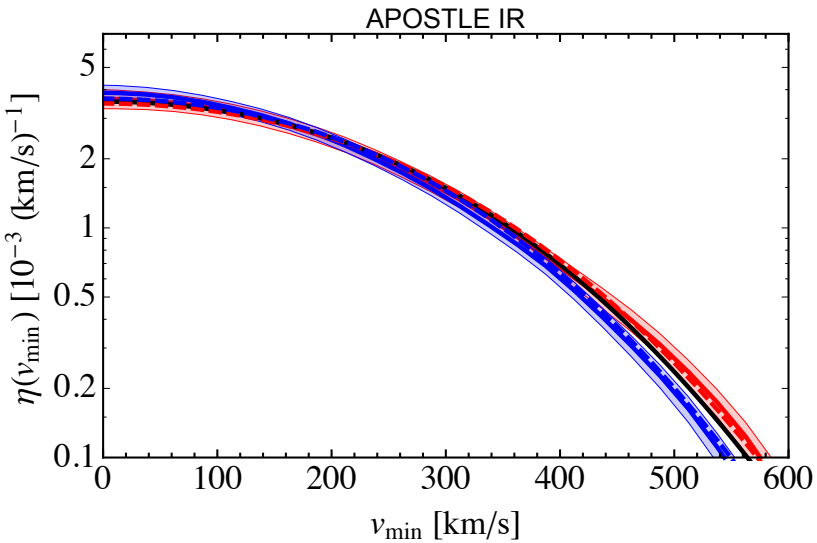

- Significant halo-to-halo scatter in the halo integrals.
- Halo integrals for the best fit Maxwellian velocity distribution (peak speed 223 – 289 km/s) fall within the 1σ uncertainty band of the halo integrals of the simulated haloes.
- Difference between simulated haloes and SHM Maxwellian due to the different peak speed of the DM velocity distribution.

The halo integral

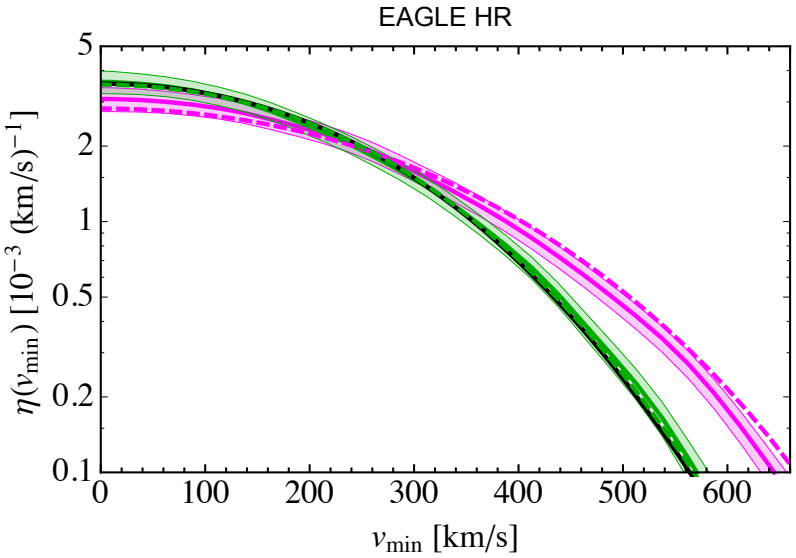

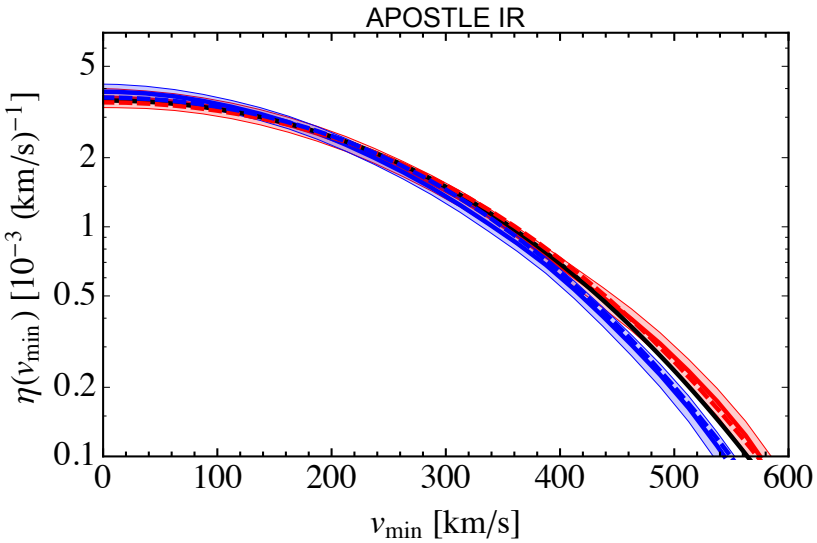

- A Maxwellian velocity distribution with a peak speed constrained by hydrodynamic simulations could be used by the community in the analysis of direct detection data.

The halo integral

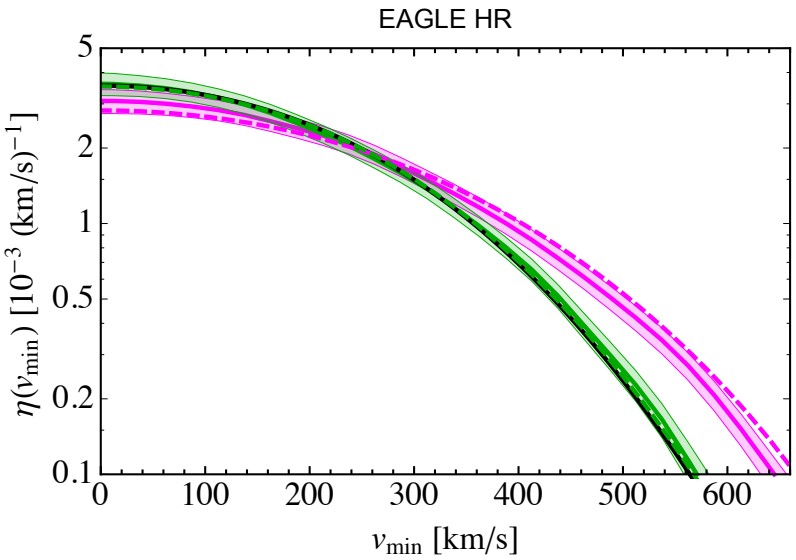

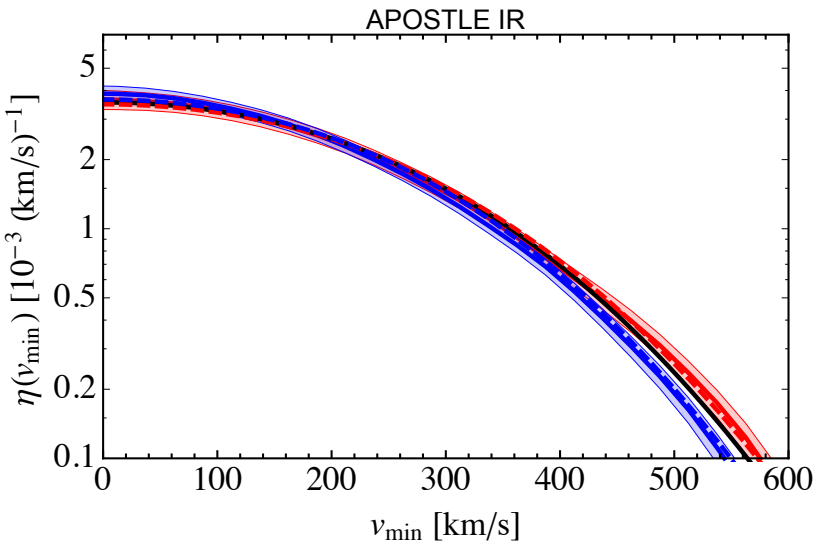

- Comparison to DMO simulations:

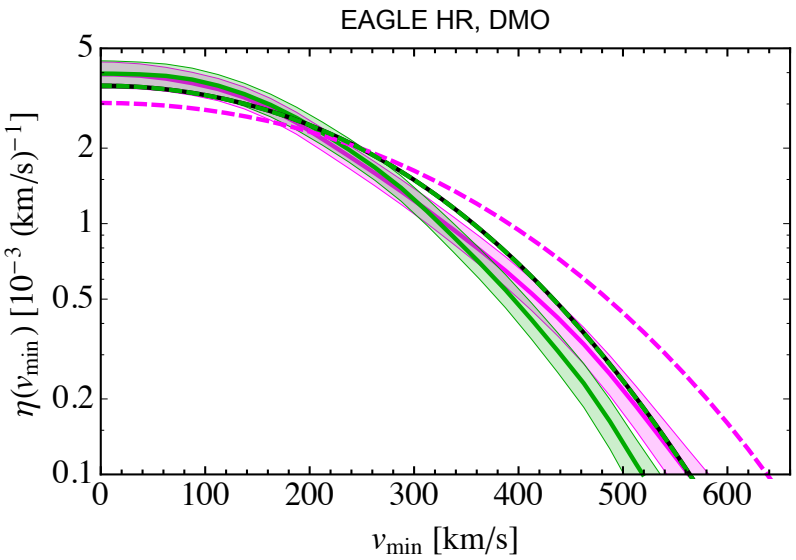

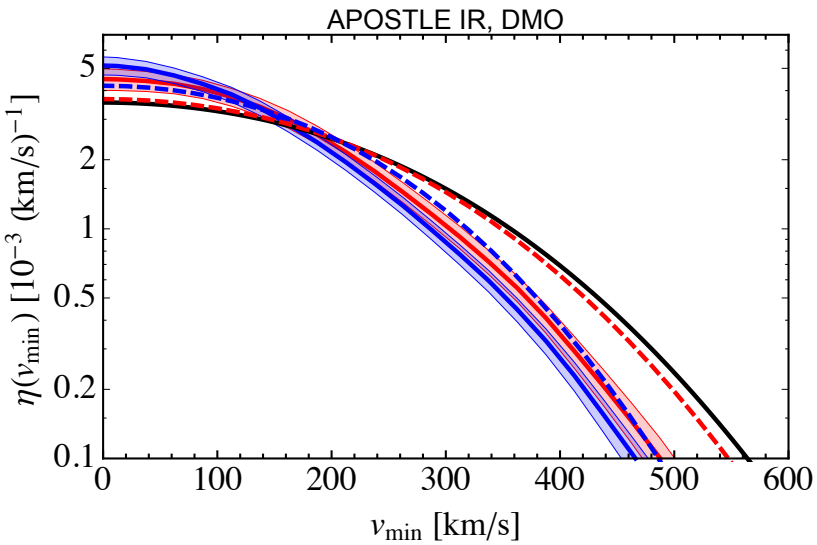

The halo integral

- Including baryons in the simulations results in a shift of the tails of the halo integrals to higher velocities with respect to the DMO case.
- Speed distributions of DMO haloes not captured well by a Maxwellian. Large deficits at the peak, and an excess at low and very high velocities compared to the best fit Maxwellian. $\Rightarrow$ Halo integrals of DMO haloes quite different from best fit Maxwellian halo integrals.

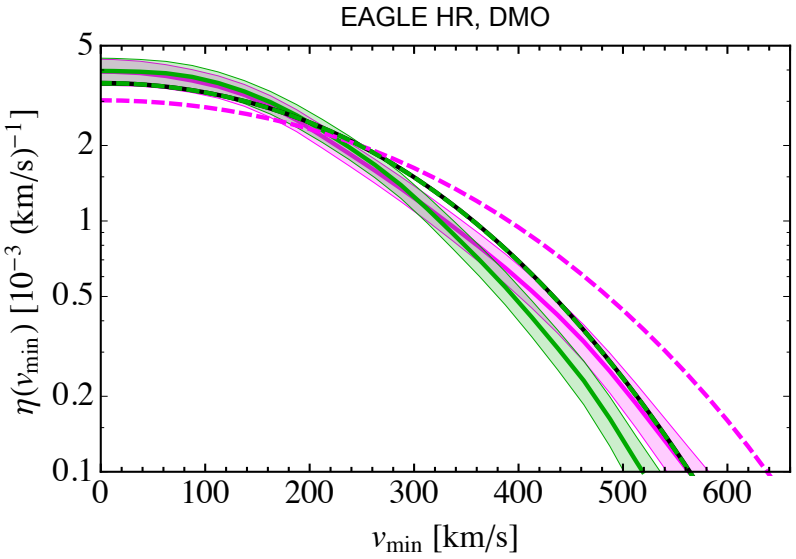

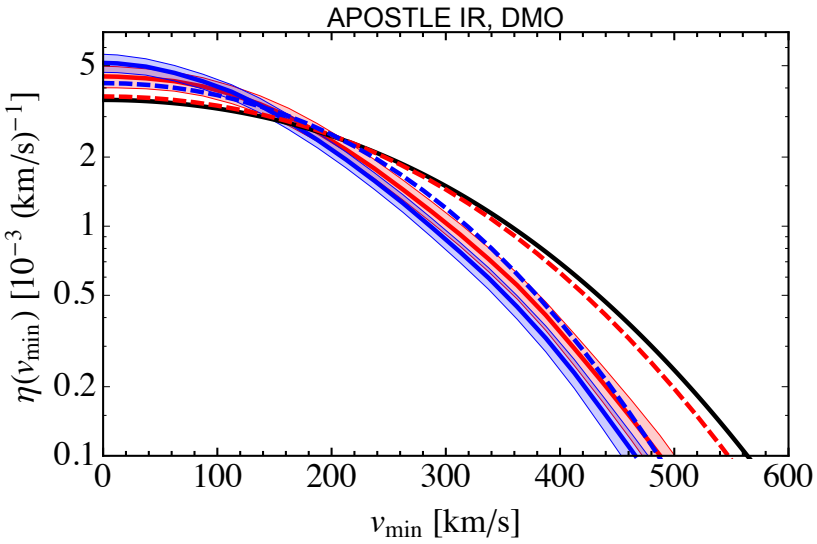

Implications for direct detection

- Assuming the SHM:

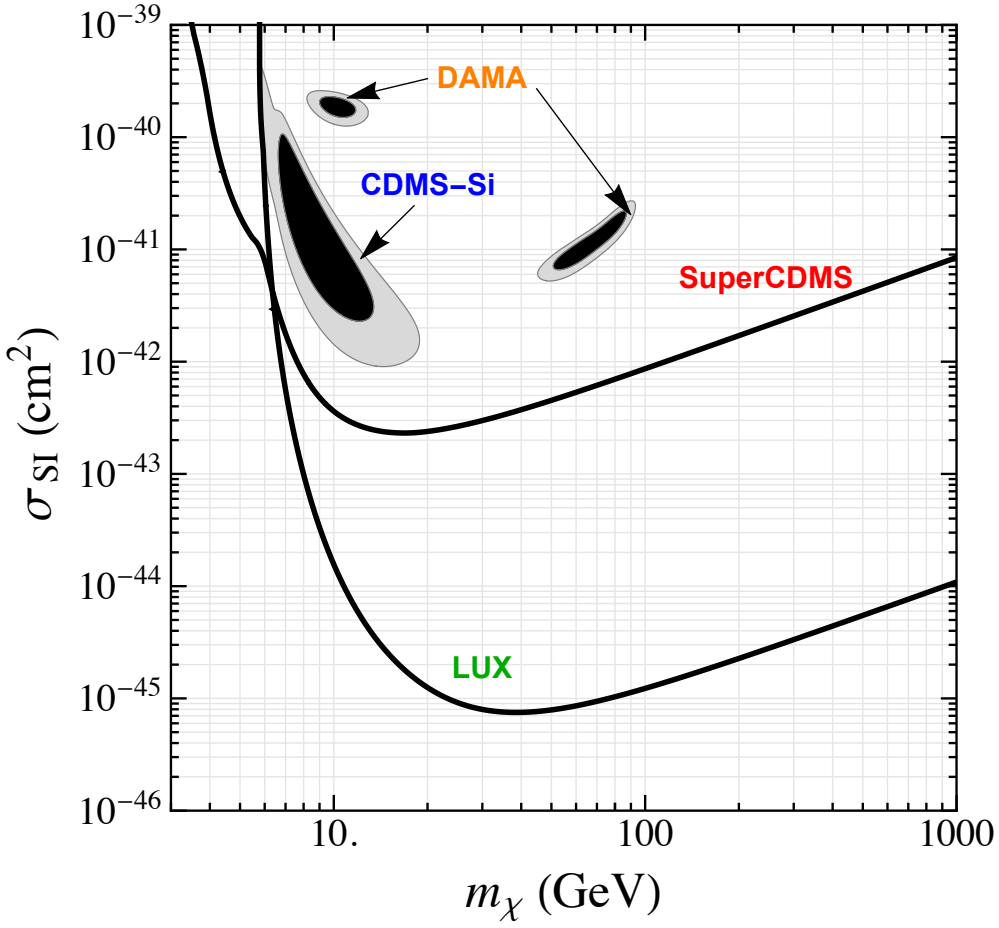

Implications for direct detection

- Comparing with simulated MW-like haloes (smallest ρ_{DM}):

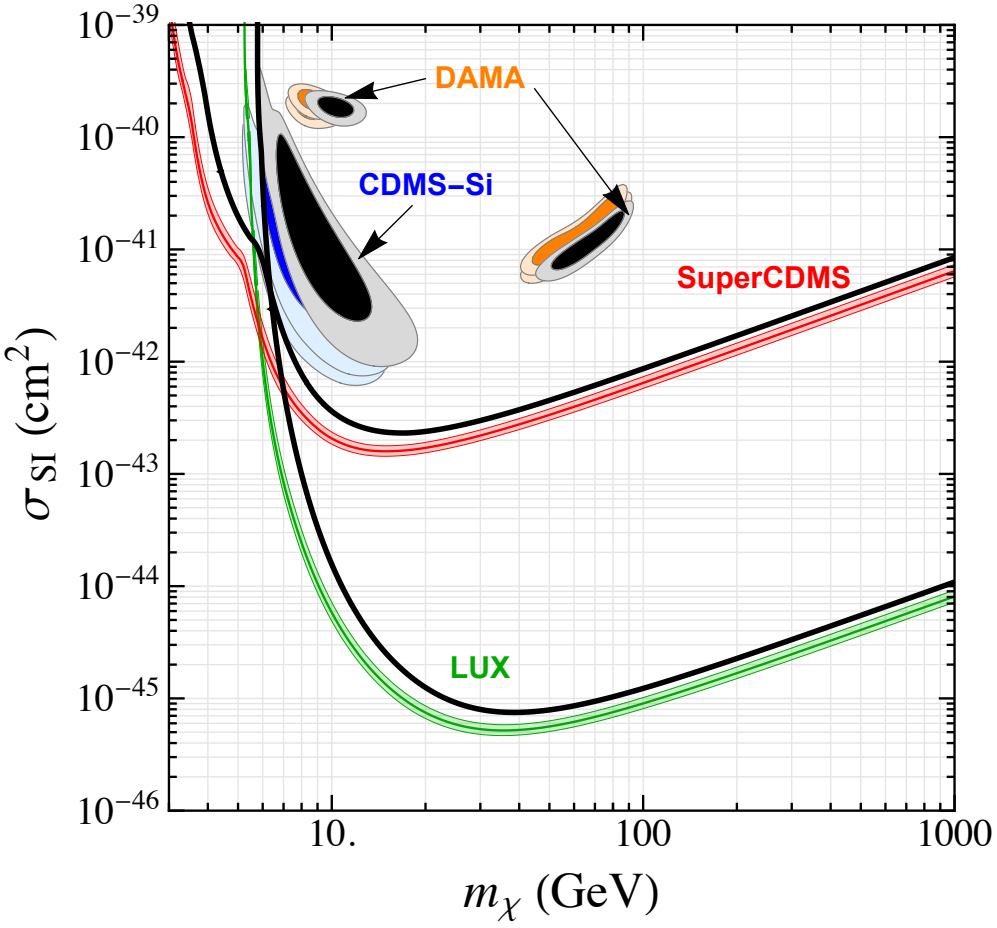

Implications for direct detection

- Comparing with simulated MW-like haloes (largest ρ_{DM}):

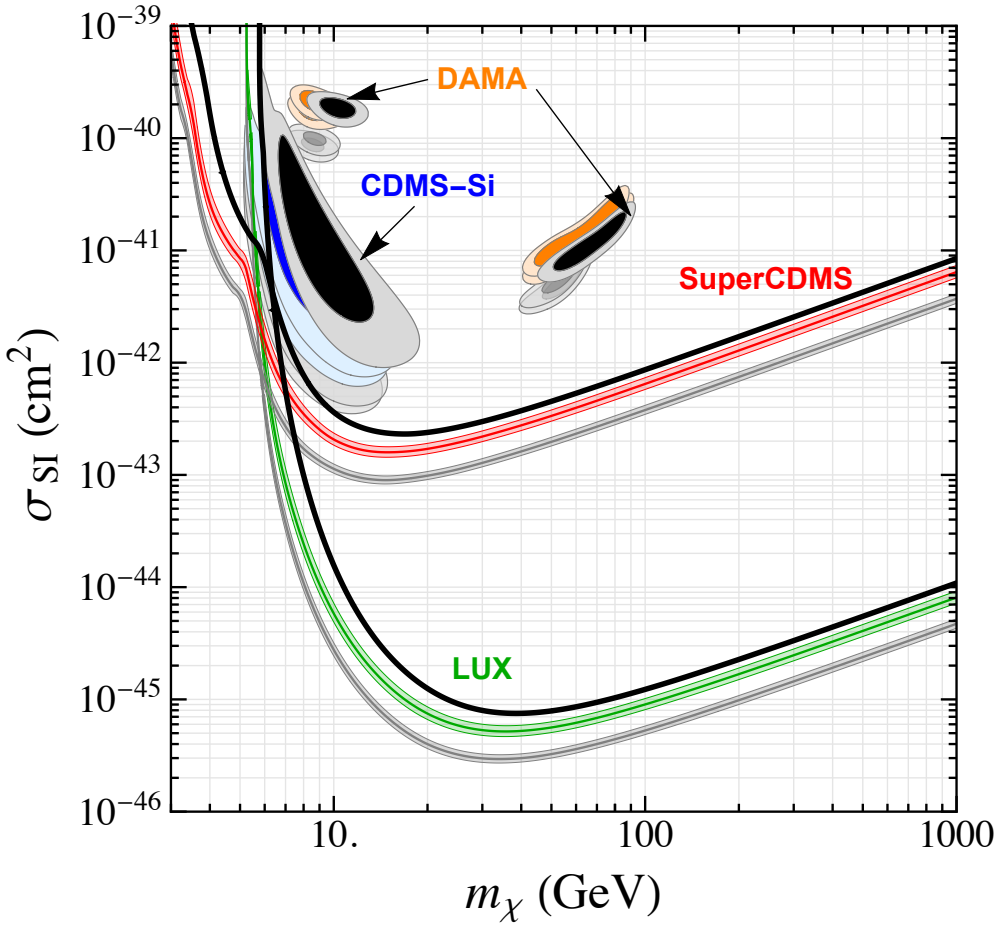

Implications for direct detection

- Comparing with simulated MW-like haloes (largest ρ_{DM}):

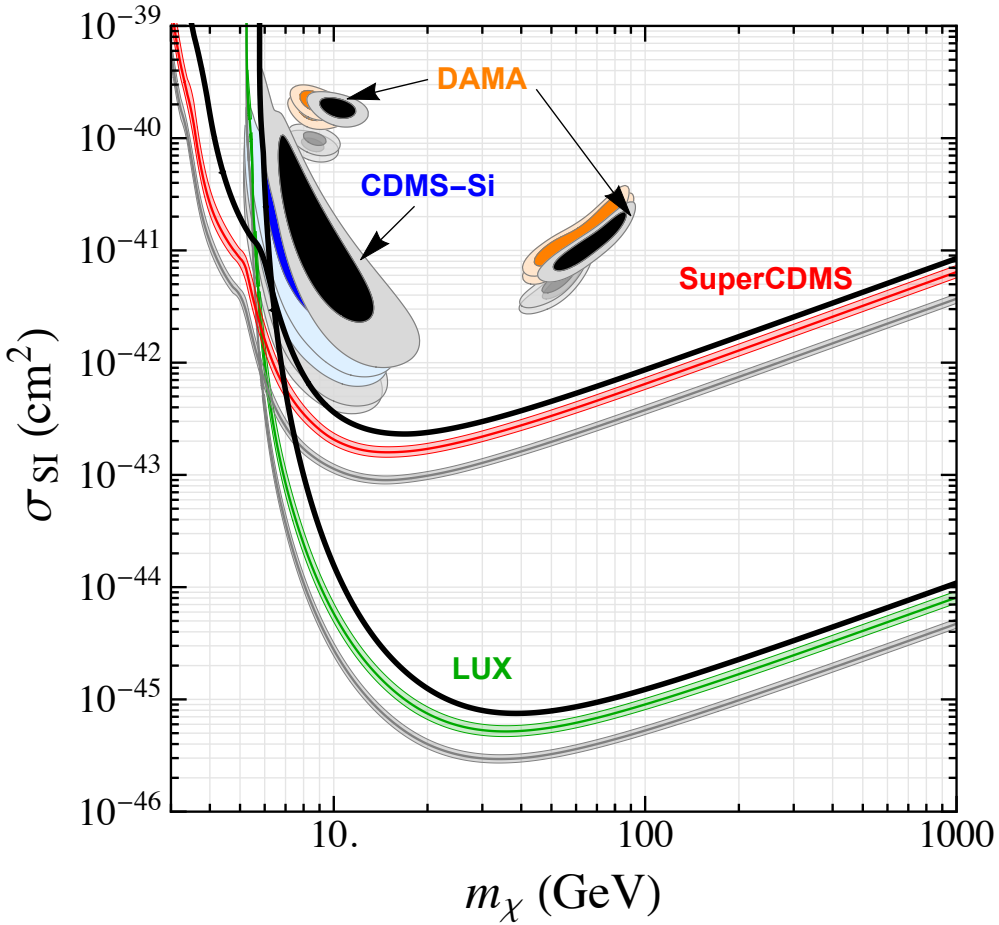

- Halo-to-halo uncertainty larger than the 1σ uncertainty from each halo.

Implications for direct detection

- Comparing with simulated MW-like haloes (largest ρ_{DM}):

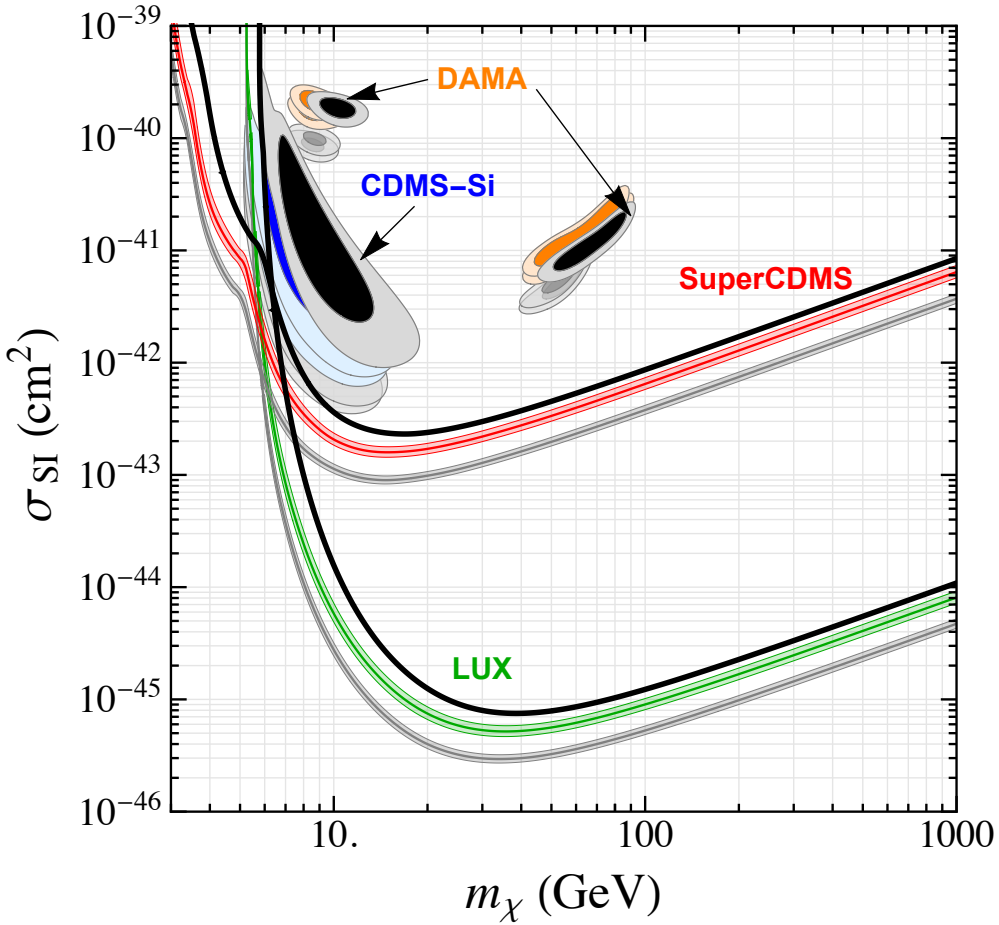

- Halo-to-halo uncertainty larger than the 1σ uncertainty from each halo.
- Overall difference with SHM mainly due to the different local DM density of the simulated haloes.

Effect of the velocity distribution

- Haloes with velocity distributions closest and farthest from SHM Maxwellian:

Fix local $\rho_{\rm DM} = 0.3$ GeV cm^{-3}

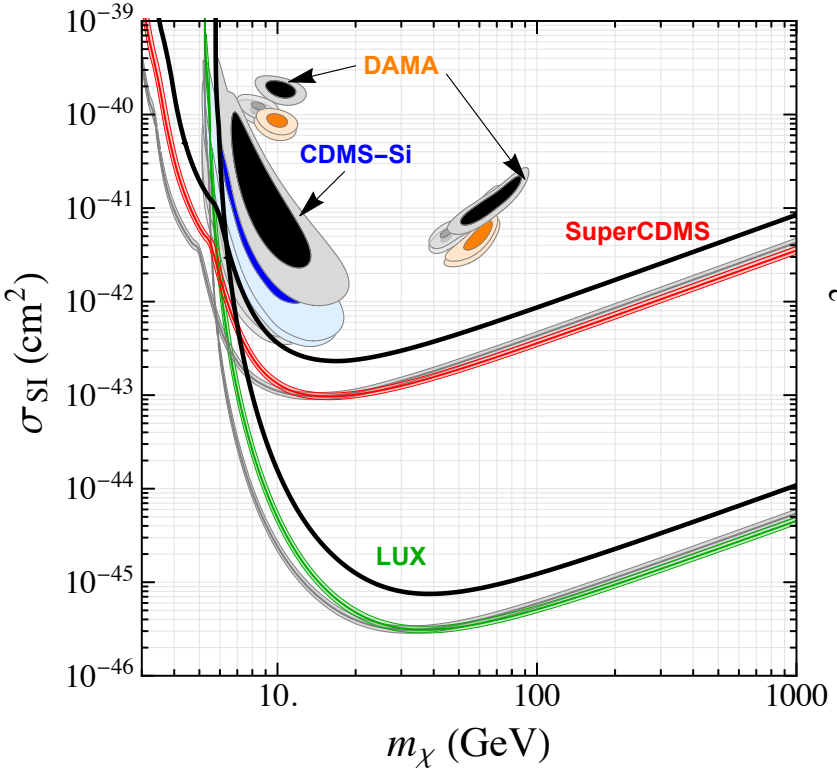

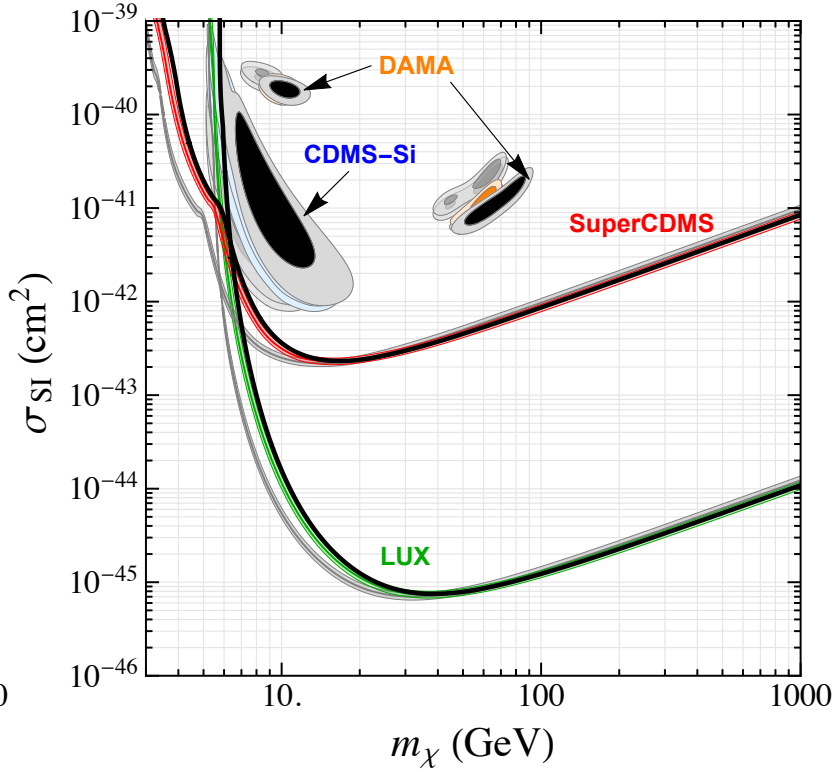

Effect of the velocity distribution

- Haloes with velocity distributions closest and farthest from SHM Maxwellian:

Fix local $\rho_{\rm DM} = 0.3$ GeV cm^{-3}

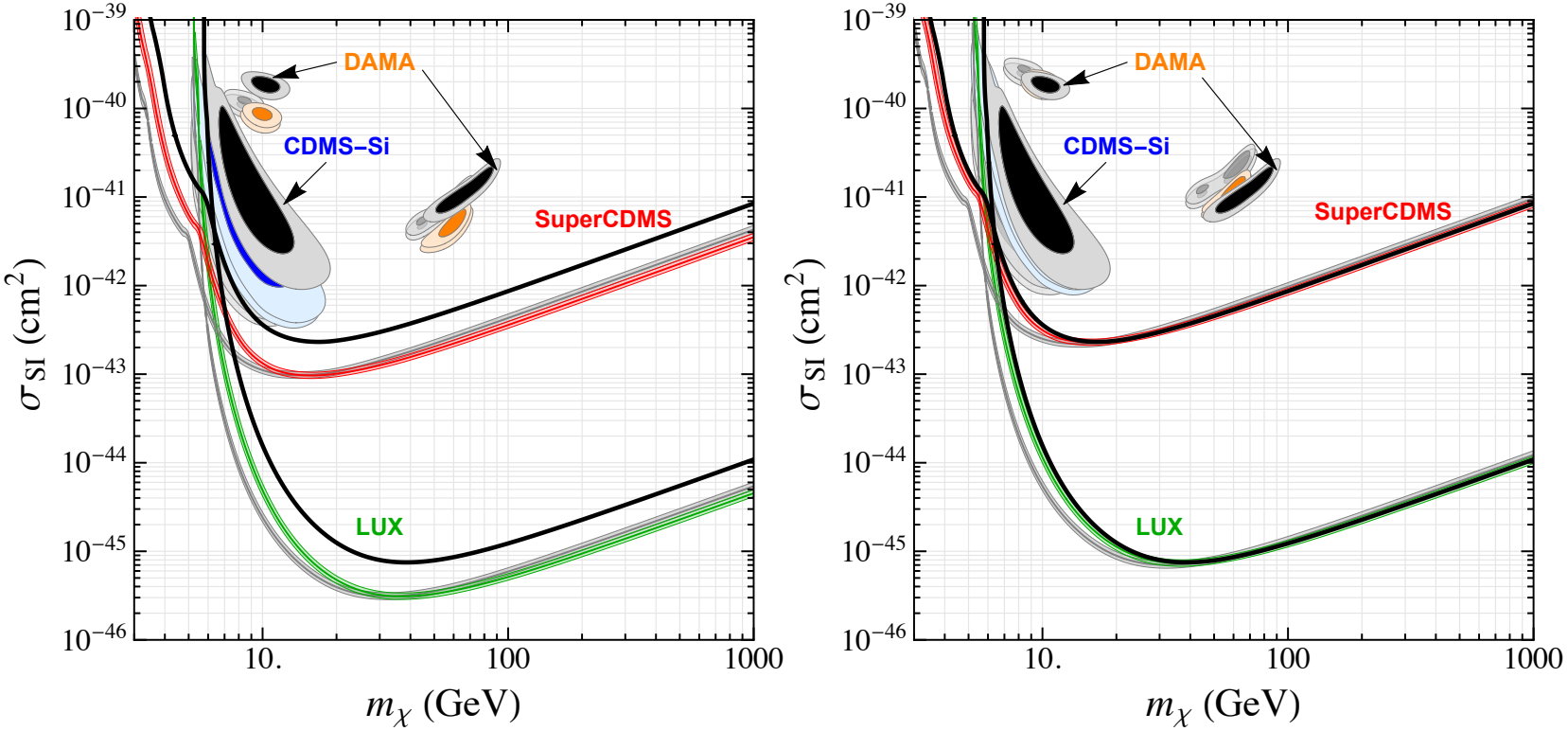

- Shift in the low WIMP mass region persists, where experiments probe the high velocity tail of the distribution.

Summary

- We identified simulated haloes which satisfy observational properties of the Milky Way, besides the uncertain mass constraint. Haloes are *MW-like* if:
  - good fit to observed MW rotation curve.
  - stellar mass in the 3σ observed MW stellar mass range.

Summary

- We identified simulated haloes which satisfy observational properties of the Milky Way, besides the uncertain mass constraint. Haloes are *MW-like* if:
  - good fit to observed MW rotation curve.
  - stellar mass in the 3σ observed MW stellar mass range.

- The local DM density: $\rho_{\rm DM} = 0.41 - 0.73$ GeV cm^{-3}. $\Rightarrow$ overall shift of the allowed regions and exclusion limits for all masses.

Summary

- We identified simulated haloes which satisfy observational properties of the Milky Way, besides the uncertain mass constraint. Haloes are *MW-like* if:
  - good fit to observed MW rotation curve.
  - stellar mass in the 3σ observed MW stellar mass range.

- The local DM density: $\rho_{\rm DM} = 0.41 - 0.73$ GeV cm^{-3}. $\Rightarrow$ overall shift of the allowed regions and exclusion limits for all masses.

- Halo integrals of MW analogues match well those obtained from best fit Maxwellian velocity distribution (with mean speed 223 – 289 km/s). $\Rightarrow$ shift of allowed regions and exclusion limits by a few GeV at low DM masses compared to SHM.

Summary

- We identified simulated haloes which satisfy observational properties of the Milky Way, besides the uncertain mass constraint. Haloes are *MW-like* if:
  - good fit to observed MW rotation curve.
  - stellar mass in the 3σ observed MW stellar mass range.

- The local DM density: $\rho_{\rm DM} = 0.41 - 0.73$ GeV cm^{-3}. $\Rightarrow$ overall shift of the allowed regions and exclusion limits for all masses.

- Halo integrals of MW analogues match well those obtained from best fit Maxwellian velocity distribution (with mean speed 223 – 289 km/s). $\Rightarrow$ shift of allowed regions and exclusion limits by a few GeV at low DM masses compared to SHM.

- Shift in the allowed regions and exclusion limits occurs in the same direction. $\Rightarrow$ compatibility between different experiments is not improved.

Additional slides

Selection criteria for MW analogues

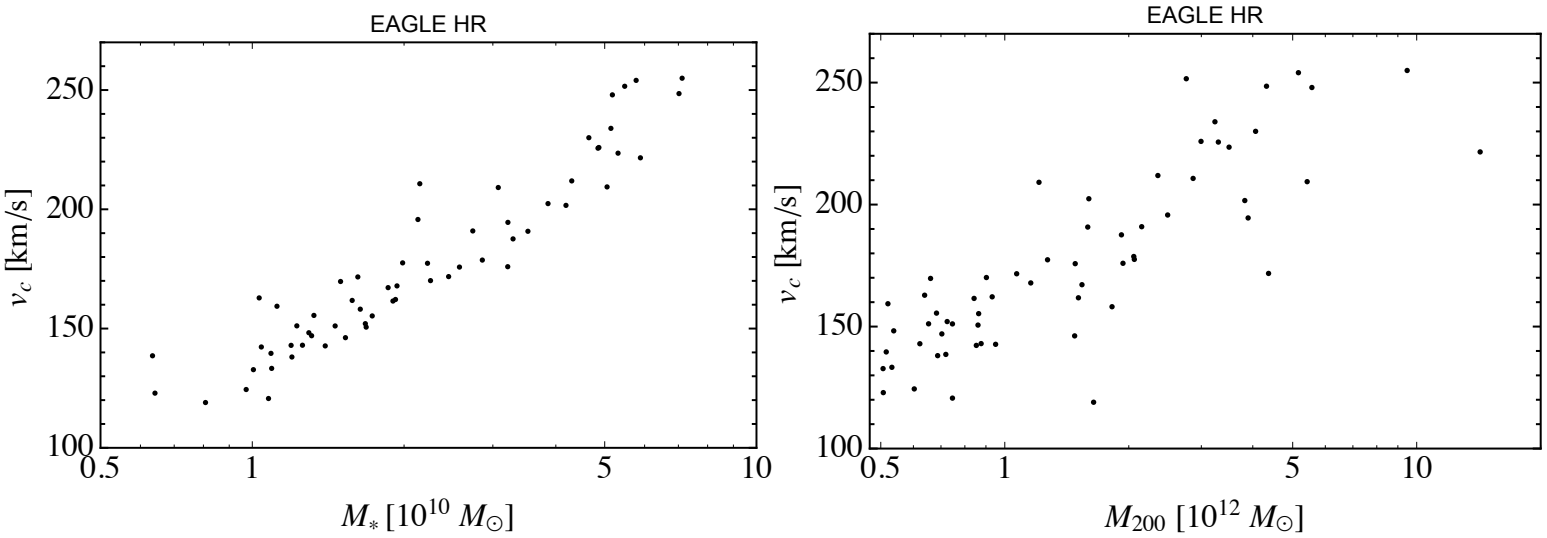

- $M_\star$ strongly correlated with v_c at 8 kpc, while the correlation of M_{200} with v_c is weaker.
- $M_\star(R < 8\ \mathrm{kpc}) = (0.5 - 0.9)M_\star$.
- $M_{\mathrm{tot}}(R < 8\ \mathrm{kpc}) = (0.01 - 0.1)M_{200}$.
- Over the small halo mass range probed, little correlation between $M_{\mathrm{DM}}(R < 8\ \mathrm{kpc})$ and M_{200}.

Velocity distribution azimuthal components

DM and stellar velocity distributions:

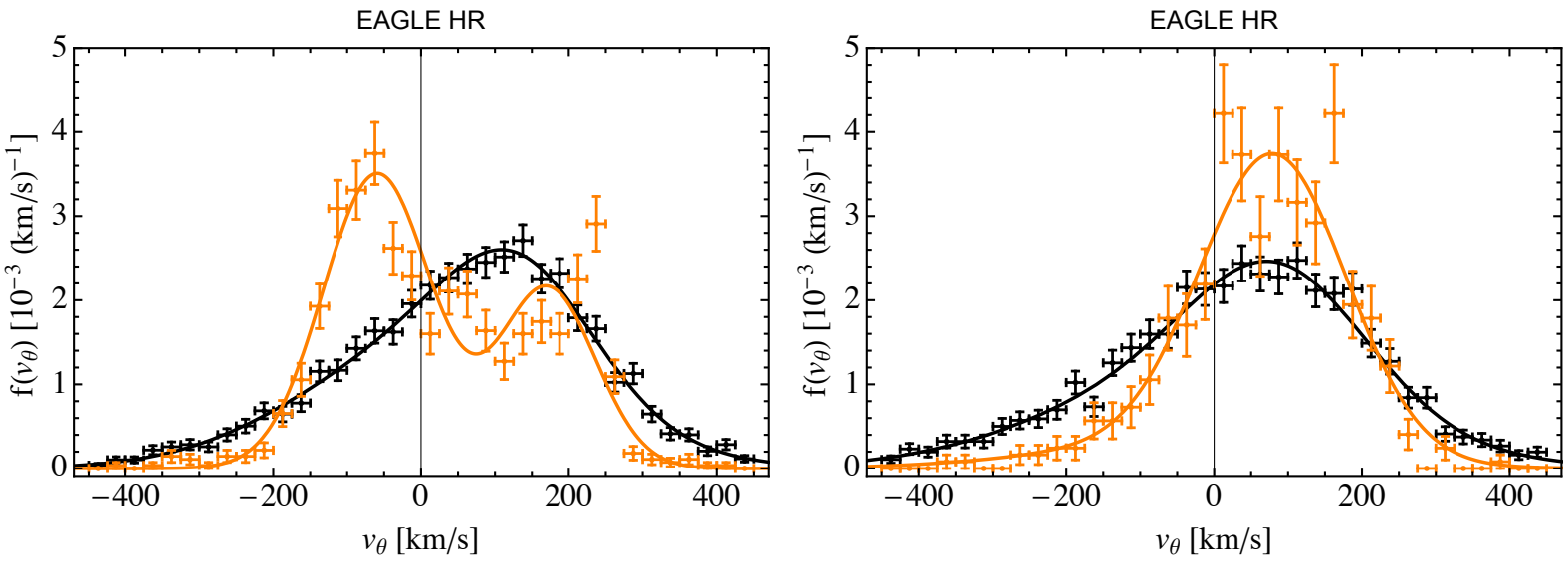

- Fit with a double Gaussian. Difference in the mean speed of second Gaussian between DM and stars is 35 km/s in the left, and 7 km/s in the right panel.
- Fraction of second Gaussian is 32% in the left panel and 43% in the right panel.

Local dark matter density

Is there an enhancement of the local DM density in the **Galactic disc** compared to the **halo**?

- Compare the the average $\rho_{\rm DM}$ in the torus with the value in a spherical shell at $7 < R < 9$ kpc.

  $\rho_{\rm DM}^{\rm torus}$ is larger than $\rho_{\rm DM}^{\rm shell}$ by:

  2 – 27% for 10 haloes,
  greater than 10% for 5 haloes, and
  greater than 20% for only two haloes.

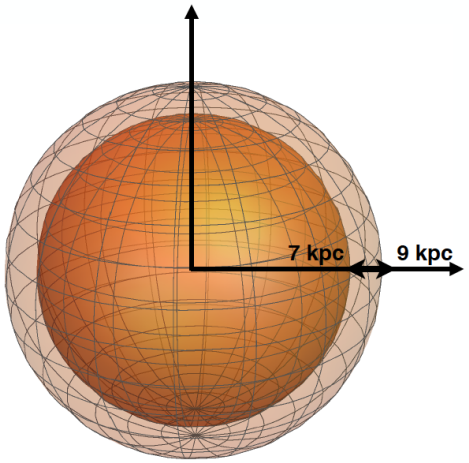

- The increase in the DM density in the disc could be due to the DM halo contraction as a result of dissipational baryonic processes.

Halo shapes

- To study the shape of the inner ($R < 8$ kpc) DM haloes, we calculate the inertia tensor of DM particles within 5 and 8 kpc. $\Rightarrow$ ellipsoid with three axes of length $a \geq b \geq c$.

- Calculate the sphericity: $s = c/a$.
  - $s = 1$: perfect sphere. $s < 1$: increasing deviation from sphericity.
  - At 5 kpc, $s = [0.85, 0.95]$. At 8 kpc, s lower by less than 10%.
  - Due to dissipational baryonic processes, DM sphericity systematically higher in the hydrodynamic simulations compared to DMO haloes in which $s = [0.75, 0.85]$.

Halo shapes

- Describe a deviation from sphericity by the triaxiality parameter:

$$T = \frac{a^2 - b^2}{a^2 - c^2}$$

- Oblate systems, $a \approx b \gg c \Rightarrow T \approx 0$.

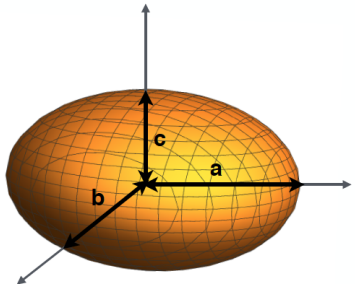

- Prolate systems, $a \gg b \approx c \Rightarrow T \approx 1$.

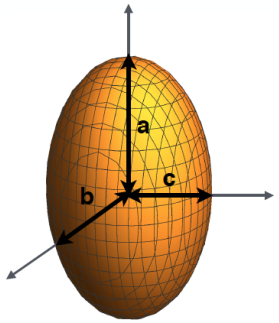

- In the hydro case, since inner haloes are very close to spherical, deviation towards either oblate or prolate is small. DMO counterparts have a preference for *prolate* inner haloes.